

Multi-scale engineering properties of tomato fruits related to harvesting, simulation and textural evaluation

Li, Zhiguo; Lv, Kun; Wang, Yuqing; Zhao, Bo; Yang, Zhibo

DOI:

[10.1016/j.lwt.2014.12.018](https://doi.org/10.1016/j.lwt.2014.12.018)

License:

None: All rights reserved

Document Version

Peer reviewed version

Citation for published version (Harvard):

Li, Z., Lv, K., Wang, Y., Zhao, B. & Yang, Z. 2015, 'Multi-scale engineering properties of tomato fruits related to harvesting, simulation and textural evaluation', *LWT - Food Science and Technology*, vol. 61, no. 2, pp. 444-451. <https://doi.org/10.1016/j.lwt.2014.12.018>

[Link to publication on Research at Birmingham portal](#)

Publisher Rights Statement:

NOTICE: this is the author's version of a work that was accepted for publication. Changes resulting from the publishing process, such as peer review, editing, corrections, structural formatting, and other quality control mechanisms may not be reflected in this document. Changes may have been made to this work since it was submitted for publication. A definitive version was subsequently published as Li, Z., Lv, K., Wang, Y., Zhao, B., Yang, Z., Multi-scale engineering properties of tomato fruits related to harvesting, simulation and textural evaluation, *LWT - Food Science and Technology* (2015), doi: 10.1016/j.lwt.2014.12.018.

General rights

Unless a licence is specified above, all rights (including copyright and moral rights) in this document are retained by the authors and/or the copyright holders. The express permission of the copyright holder must be obtained for any use of this material other than for purposes permitted by law.

- Users may freely distribute the URL that is used to identify this publication.
- Users may download and/or print one copy of the publication from the University of Birmingham research portal for the purpose of private study or non-commercial research.
- User may use extracts from the document in line with the concept of 'fair dealing' under the Copyright, Designs and Patents Act 1988 (?)
- Users may not further distribute the material nor use it for the purposes of commercial gain.

Where a licence is displayed above, please note the terms and conditions of the licence govern your use of this document.

When citing, please reference the published version.

Take down policy

While the University of Birmingham exercises care and attention in making items available there are rare occasions when an item has been uploaded in error or has been deemed to be commercially or otherwise sensitive.

If you believe that this is the case for this document, please contact UBIRA@lists.bham.ac.uk providing details and we will remove access to the work immediately and investigate.

Accepted Manuscript

Multi-scale engineering properties of tomato fruits related to harvesting, simulation and textural evaluation

Zhiguo Li , Kun Lv , Yuqing Wang , Bo Zhao , Zhibo Yang



PII: S0023-6438(14)00794-4

DOI: [10.1016/j.lwt.2014.12.018](https://doi.org/10.1016/j.lwt.2014.12.018)

Reference: YFSTL 4335

To appear in: *LWT - Food Science and Technology*

Received Date: 4 July 2014

Revised Date: 1 December 2014

Accepted Date: 2 December 2014

Please cite this article as: Li, Z., Lv, K., Wang, Y., Zhao, B., Yang, Z., Multi-scale engineering properties of tomato fruits related to harvesting, simulation and textural evaluation, *LWT - Food Science and Technology* (2015), doi: 10.1016/j.lwt.2014.12.018.

This is a PDF file of an unedited manuscript that has been accepted for publication. As a service to our customers we are providing this early version of the manuscript. The manuscript will undergo copyediting, typesetting, and review of the resulting proof before it is published in its final form. Please note that during the production process errors may be discovered which could affect the content, and all legal disclaimers that apply to the journal pertain.

Multi-scale engineering properties of tomato fruits related to harvesting, simulation and textural evaluation

Zhiguo Li^{1,2*}, Kun Lv¹, Yuqing Wang¹, Bo Zhao¹ and Zhibo Yang¹

1. School of Mechanical and Power Engineering, Henan Polytechnic University, 454003 Jiaozuo, China

2. School of Chemical Engineering, University of Birmingham, Edgbaston, Birmingham B15 2TT, UK

*Corresponding author at: Tel. /fax: +0086-391-3983223. E-mail address: lizhiguo0821@163.com

Abstract

In this study, multi-scale engineering properties related to the harvesting, simulation and textural evaluation of two tomato cultivars at six ripening stages were simultaneously investigated. A potential ripening scale based on the ratio of R:G:B for a given ripening stage was suggested. The geometric mean diameter was most closely correlated with the fruit mass. Tomato fruit feature an irregular shape and asymmetric internal structure at the macro-scale, non-unique tissue thickness at the meso-scale and an irregular change of size, shape and arrangement of single cells at the micro-scale. The hardness and shear strength of fruit at different scales and the single cell mechanics varied with the fruit ripening stage but not the chosen cultivars. The contribution of exocarp to the hardness of whole fruit gradually increased with fruit ripeness. The hardness and shear strength of fruit tissues and the fruit's single cells varied between 0.37 and 2.25 MPa and 0.04 and 11.58 MPa, respectively. This puncture experimental method is well-suited to measure the hardness and shear strength of tomato fruit at different scales and single tomato cell mechanics.

Keywords: *Solanum lycopersicum*; Tomato cell; Multi-scale biomechanics; Ripeness; Puncture test

1 Introduction

Numerous large-scale tomato-growing farms are in operation worldwide because tomatoes are a component of the diet of millions of people. Because the harvesting season is short and harvesting work is concentrated during a brief period of time, labor shortages tend to limit the farm acreage (Tanigaki, Fujiura, Akase, & Imagawa,

24 2008). Additionally, given the long distance between farms and sale markets, the design and development of
25 intelligent equipment for mechanical harvesting, packaging and transport have received increasing attention
26 (Kondo, Yata, Taniwaki, Tanihara, Monta, & Kurita, 2007; Li, Li, Yang, & Wang, 2013a). Furthermore, fruits with
27 a distinct multi-scale nature are very susceptible to mechanical damage during postharvest handling; thus,
28 multi-scale modeling, internal damage simulation and postharvest textural evaluation are extremely important
29 (Genard et al., 2007; Mebatsion, Verboven, Ho, Verlinden, & Nicolai, 2008; Ghysels, Samaey, Van Liedekerke,
30 Tijssens, Ramon, & Roose, 2010; Ho et al., 2013). Determining the multi-scale engineering properties of tomato
31 fruits is essential to achieve these aims.

32 Some engineering properties of tomato fruits have been previously investigated. Arazuri et al. (2007), Li et al.
33 (2011) and Sirisomboon et al. (2012) reported the geometric and mechanical macro-properties of tomato fruits at
34 three different stages of ripeness (Arazuri, Jaren, Arana & Perez De Ciriza, 2007; Li, Li, & Liu, 2011;
35 Sirisomboon, Tanaka, & Kojima, 2012). Hetzroni et al. (2011) and Li et al. (2012a) determined the physical and
36 biomechanical properties of the peels and internal tissues of five tomato cultivars at the meso-scale (Hetzroni,
37 Vana, & Mizrach, 2011; Li, Li, Yang, Liu, & Xu, 2012a). Rancic et al. (2010) presented the geometric
38 characteristics of the fruits and tissues of two tomato genotypes during fruit development (Rancic, Quarrie, &
39 Pecinar, 2010). Bargel and Neinhuis (2005) focused on the morphology and biomechanics of skin and
40 enzymatically isolated the cuticular membranes of three tomato cultivars during fruit growth and ripening (Bargel
41 & Neinhuis, 2005).

42 Tomato fruits are hierarchically structured at the macro-scale, consisting of different tissue types at the
43 meso-scale, each of which is a highly structured arrangement of cells at the micro-scale (Li & Thomas, 2014a, b).
44 However, some important engineering parameters for multi-scale modeling and simulation, such as the geometry
45 of the whole fruit, the size and shape of the different tissues, the cell sizes in each tissue and the multi-scale
46 biomechanics, have never been fully determined for single fruit, even though these characteristics significantly

47 differ. Additionally, little is known about the relationship between different physical parameters and the
48 micro-mechanics at the cell level. Therefore, a clear gap in knowledge exists between the published data on fruit
49 engineering properties and the necessary data related to intelligent harvesting, multi-scale simulation and
50 postharvest textural evaluation. The objective of this study was to investigate the multi-scale engineering
51 properties of tomato fruits.

52 **2 Materials and Methods**

53 **2.1 Materials**

54 The experiments were conducted in May 2014 at Henan Polytechnic University. Fruits of two tomato
55 varieties, *Fendu 79* and *Omeiya 333*, were used for this study. The tomato fruits were hand-harvested from the
56 Jiaozuo *Manfeng* Vegetable Planting Base at six ripening stages (green, breaker, turning, pink, light red and red)
57 according to the USDA standards (USDA, 1991), as shown in Fig. 1a. These fruits were inspected to ensure that
58 they were not damaged or infested with insects prior to transport to the laboratory. Subsequently, the fruits'
59 surfaces were manually cleaned and dried. In total, 60 tomato fruits (5 samples \times 2 varieties \times 6 ripening stages)
60 were used to measure the multi-scale geometric characteristics, and 12 tomato fruits (1 sample \times 2 varieties \times 6
61 ripening stages) were used for the puncture test.

62 **2.2 Quantification of ripeness**

63 One tomato fruit was randomly selected from each ripening stage (green, breaker, turning, pink, light red and
64 red). These tomatoes were grouped and placed on a blank paper with the support of wedges, as shown in Fig. 1a.
65 A JPEG photo of tomato fruits from front view was then obtained using a digital camera (Canon 95IS, Photo size:
66 3648 \times 2736 pixels). Subsequently, ten pixel points were randomly grabbed from each tomato fruit using a color
67 picker software (ColorPix version 1.1, http://www.colorschemer.com/colorpix_info.php). The three primary color
68 values of grabbed points, namely Red-Green-Blue (RGB), were then based on the automatic transformation
69 provided by the software.

70 2.3 Multi-scale geometric characteristics measurement

71 The sampled fruits were labeled and then cut into halves with a sharp knife along the stem-blossom axis (Fig.
72 2a). One half of each fruit was cut again along the equatorial axis (Fig. 2b). Further descriptions of the tomato
73 fruit anatomy are given in Thomas (1996). The following were measured using an electronic digital caliper (to an
74 accuracy of 0.01 mm): height above the fruit's equatorial axis (section) (H_1); height below the fruit's equatorial
75 axis (H_2); diameter of the equatorial section (D_f); maximum thickness (W_{max}), minimum thickness (W_{min}),
76 middle thickness of the mesocarp tissue (W_{mid}); thickness of the septa tissue (W_s); and columella diameter (D_{ct}).
77 Subsequently, rectangular tissue blocks, including the exocarp and some of the adhering mesocarp, were excised
78 and soaked in boiling water for 5 minutes. The exocarp samples remained after the mesocarp was carefully
79 scraped off using a razor blade. The thicknesses of the exocarp samples (W_e) were then measured with an
80 electronic digital caliper.

81 As shown in Fig. 2a, some tissue blocks, including the exocarp and mesocarp and some columella tissue
82 blocks, were excised from the sample zones shown in the other half of the fruits. The mesocarp and columella
83 tissue samples were cut into thin rectangular slices (length \times width \times thickness: 15 mm \times 10 mm \times 0.5 mm) using
84 a razor blade. The exocarp samples remained after the adhering mesocarp sample was carefully scraped off. These
85 tissue samples were made into temporary mounts and then vertically observed using a Belona BL-SM1280
86 biological microscope that featured a 130w electronic eyepiece (Captured image size: 1280x1024 pixels,
87 Resolution: 96 PPI). The diameters (D_c) (Fig. 2c) of cells in different tomato fruit tissue types were measured with
88 a virtual cross ruler using the image processing software *Future WinJoe* of the eyepiece (Assumption: spherical
89 cell). The reported values of the cell geometric characteristics are the means of 5 cells in corresponding tissues.
90 The multi-scale geometric characteristics of tomato fruits were measured within 24 h of sampling at room
91 temperature ($23 \pm 1^\circ\text{C}$, 56-58 % RH).

92 2.4 Puncture test

93 The puncture test, which involves compression and shear components, is one of the most widely used
94 methods for the objective measurement of the biomechanics of fruits. The compression component results
95 from the compression effect of a probe tip plate that contacts an area of planar tissue at a puncture point. The
96 peak puncture force of the biomaterial (e.g. fruit, tissue and cell) at a unit compression area in a puncture test
97 has been considered to represent the biomaterial hardness in studies of apple fruit by Harker et al. (2002) and
98 studies of tomato fruit by Biswas et al. (2014) (Harker, Maindonald, Murray, Gunson, Hallett & Walker,
99 2002; Biswas, East, Hewett, & Heyes, 2014). The shear component results from the shear effect of the probe
100 tip edge, which contacts a toroidal tissue area at a puncture depth. The peak puncture force of the biomaterial
101 (e.g. fruit, tissue and cell) at a unit shear area in a puncture test is considered the shear strength of the
102 biomaterial.

103 The puncture test of fruits and their exocarp, mesocarp and columella tissues were used to determine the
104 multi-scale hardness and shear strength of tomato fruits as related to texture evaluation. The tests utilized a GY-4
105 manual fruit sclerometer with a 3.5-mm diameter flat-head stainless steel cylindrical probe (Fig. 3a). The
106 compression speed was approximately 1 mm/s, which was measured using a DM6236P Digital Velometer
107 (Resolution: 0.2 mm/s). A 5-mm diameter counter bore was created in the base plate of the manual test stand. The
108 test was conducted as follows:

109 First, a tomato fruit was placed on a base plate with the stem-blossom axis parallel to the flat plate. Six points
110 (Fig. 3-b1) on the equatorial section of the fruit were punctured to a depth of 10 mm. The fruit hardness, P_{th} , was
111 calculated with 6 points (replications) using the equation in Fig. 3-c1, and its mean value is reported.

112 Second, the centerlines of the puncture probe and the counter bore were adjusted on the same straight line.
113 The conjoint exocarp and mesocarp, mesocarp and columella tissues were cut into several standard cuboid
114 samples (Fig. 3-b2, b3) and then fully punctured to counter bore. The tissue sample thickness, d_2 , was measured
115 using an electronic digital caliper. The hardness, P_{th} , and shear strength, σ_{tf} , of the mesocarp and columella tissues

116 were calculated with 3 samples (replications) using the equation in Fig. 3-c2, and their mean values are reported.
117 Because the puncture resistance of the exocarp tissue always exceeded that of the mesocarp tissue (Li et al.,
118 2012a), the peak puncture force of the exocarp tissue was retained (obtained by the fruit sclerometer) when the
119 conjoint exocarp and mesocarp sample was punctured (Fig. 3-b2). Each tissue (e.g., exocarp, mesocarp or
120 columella) consists of cells. To simplify the later analysis and the multi-scale modeling in future, we assumed that
121 i) the hardness or shear strength values of each tissue and its single cells are the same during the puncture test,
122 namely $P_{th}=P_{ch}$, $\sigma_{tf}=\sigma_{cf}$; and that ii) the hardness and the shear strength for single cells in each tissue are
123 approximations.

124 Third, the tissue was assumed to consist of multilayers of regularly arranged cells (Fig. 3-b3). The mean or
125 maximum compression force applied to a single cell, F_{ch} , and the mean shear force applied to a single cell, F_{cf} ,
126 were calculated using 3 samples (replications) and the equation in Fig. 3-c3, and their mean values are reported.
127 The labels n_1 and n_2 are the numbers of cells compressed and sheared by the probe during the tissue puncture test,
128 respectively. n'_1 represents the number of first-layer cells compressed directly by the probe.

129 2.5 Statistical analysis

130 The results were analyzed for statistical significance using a variance analysis in the SAS9.1 software, with a
131 significance level of $\alpha=0.05$.

132 3 Results and Discussion

133 3.1 Ripening stage

134 According to the United States Standards for Grades of Fresh Tomatoes, the six ripening stages of tomato
135 fruits include green, breaker, turning, pink, light red, and red. “Green” indicates a completely green color on the
136 fruit surface; “breaker” indicates fruit that is not fully green and features a red area on the surface (< 10 %); more
137 than 10% but less than 30% of the surface of “turning” fruit is red; more than 30% but less than 60% of the
138 surfaces of “pink” fruit are red; more than 60% but less than 90% of the surfaces of “light red” are red; and “red”

139 denotes fruit whose surfaces are more than 90% red. The above ripeness classification is a simple qualitative
140 recognition method. The RGB values and their standard deviations corresponding to six ripening stages are
141 presented in Fig. 1b. A ripening scale based on the ratio of R:G:B obtained from quantifying the RGB value has
142 been proposed. The standard deviations showed that the three primary colors, RGB, fluctuated for a given
143 ripening stage. The RGB threshold values of different ripening stages contribute to quantitative recognition and
144 are vital for the color-sorting device of a tomato harvester and other quality detection systems (Li, Kan, Tan,
145 Zhang, Sui, & Chen, 2012b).

146 As the fruit ripened, the color gradually changed from green to red, mainly because of the increased lycopene
147 and decreased chlorophyll content in fruit tissues (Salunkhe et al., 1974), while the hardness gradually decreased
148 due to multiple coordinated processes, including the disassembly of polysaccharide in the primary cell wall and
149 middle lamella and transpirational water/turgor loss (Saladie, Jadav, & Yu, 2007). Therefore, tomato fruits at the
150 pink and light-red stages are considered optimal for harvesting due to the long distance transportation from farms
151 to markets and thus are the most important fruit for biomechanical measurements and simulation analysis. After
152 quantitative transformation, the R, G, and B values \pm standard deviations were 150 ± 31 , 110 ± 27 , and 70 ± 18 for
153 pink tomatoes and 152 ± 15 , 78 ± 13 , and 54 ± 9 for light red tomatoes, respectively.

154 **3.2 Multi-scale geometry**

155 **3.2.1 Fruit**

156 The height, diameter and mass of the two tomato cultivars varied from 51.75-61.86 mm, 58.56-74.19 mm
157 and 89.49-224.56 g, respectively, which further illustrated that the shapes of tomato fruits are irregular. Based on
158 these data, the finger grasping stroke and the surface width should exceed 61.86 mm and 37.09, respectively, for
159 the two-finger harvesting robot designed by Monta, Kondo, & Ting. (1998) and Li et al. (2013a). The centrifugal
160 force of the separation device of the tomato harvester designed by Li et al. (2012b) should be sufficient to separate
161 the largest (224.56 g) fruits from tomato stems; and the grid gap of its conveyor chain should not exceed 51.75

162 mm. Fig. 4a shows the height and diameter of the two tomato cultivars at the six ripening stages. The height and
163 diameter of the two tomato cultivars at the six ripening stages did not significantly differ because the fruits had
164 already been selected during manual harvesting. Therefore, the macro size of the fruits will not affect the
165 following physical-mechanical characteristics in section 3.3 and 3.4 .

166 Fig. 4b shows the fruit heights above and below the equatorial section. The height above the equatorial
167 section of tomato fruits was 21.93 ± 3.73 mm, and the height below the equatorial section was 33.47 ± 4.03 mm. The
168 fruit height below the equatorial section was larger than the height above the equatorial section. This finding
169 further illustrates that the macro-structure of tomato fruits is asymmetrical and that consistent, significant
170 differences in the fruit mechanics can be expected during quasi-static compression, dynamic impact or free drop
171 experiments from different force action points, as reported by Li et al. (2011) and Van Linden, Scheelinck, Desmet,
172 & De Baerdemaeker. (2006). Therefore, a real multi-scale fruit model is more valuable for a mechanical handling
173 (such as harvesting, transporting and packaging) simulation than an ideal model.

174 Fig. 4c shows the regression relationships between the fruit mass and height and the equatorial diameter and
175 geometric mean diameter. The fruit mass and its geometric mean diameter most closely correlated according to the
176 determination coefficient, R^2 . of the regression functions ($n=12$). When a robot harvests fruit, the stable grasp
177 force of fingers needs to be calculated from the friction coefficient and mass (Chen, Hasegawaa, & amashita, 2006;
178 Li et al., 2013a), but the fruit mass cannot be directly measured with a balance. According to the Fig. 4c, the
179 geometric mean diameter can be considered as the most accurate parameter for predicting the fruit mass for robot
180 harvesting.

181 3.2.2 Tissue

182 The results of the two-factor analysis of variance indicated significant differences in the thickness of the
183 exocarp tissue, W_e , but no significant differences in the other geometric parameters of the tissues of the two
184 tomato cultivars. Furthermore, the measured geometric parameters of the tissues did not correlate with ripeness.

185 This lack of correlation may have been due to the fact that the geometric sizes of tomato fruits no longer rapidly
186 grow as a result of insignificant cell enlargement 5~8 weeks after anthesis, when the tomato fruit has accumulated
187 the majority of its final mass from the mature green stage (Thomas, 1996).

188 The thicknesses of *Fendu 79* and *Omeiya 333* exocarp tissue were 0.17 ± 0.02 mm and 0.14 ± 0.03 mm,
189 respectively. The thicknesses (W_{max} , W_{min} and W_{mid}) of the mesocarp tissue, the thickness (W_s) of the septa
190 tissue and the columella diameter (D_{ct}) were 7.56 ± 1.02 mm, 5.17 ± 0.63 mm, 4.17 ± 0.84 mm, 6.38 ± 0.62 mm and
191 9.76 ± 0.75 mm, respectively, which further illustrated non-unique tissue thickness at the meso-scale. All of the
192 exocarp tissues were thicker than those examined by Hetzroni et al. (2011) and Bargel & Neinhuis (2005). Lahaye,
193 Devaux, Poole, Seymour, & Causse (2013) proposed that tomato pericarp tissue thickness ranged from 5.2 to 9.3
194 mm. These measured geometric data are essential for tissue geometric modeling in multi-scale simulations but
195 have not been fully determined for individual fruit cultivars. The measured geometric sizes of tissues demonstrate
196 the complex internal structural characteristics of tomato fruits. Structural failure has been suggested as another
197 type of mechanical damage to tomato fruits in addition to the failure of tissues (Li, Li, Yang, & Liu, 2013b).

198 3.2.3 Cell

199 The cell diameters in different types of tissues of the two tomato cultivars at six ripening stages are presented
200 in Fig. 5a. The sizes of cells in the mesocarp and columella tissues significantly varied, as illustrated by several
201 large standard deviation values. The results of the analysis of variance show that the two tomato cultivars and the
202 three tissue types (e.g. exocarp, mesocarp, and columella) markedly affected the cell diameter, D_c . The mean cell
203 diameters of the exocarp, mesocarp and columella tissues were 32 μm , 327 μm and 340 μm , respectively, for
204 *Fendu 79* tomato fruits and 35 μm , 389 μm and 429 μm , respectively, for *Omeiya 333* tomato fruits.

205 Fig. 5b shows a picture of the microstructure of the exocarp, mesocarp and columella tissues of *Fendu 79*
206 tomato fruits at the breaker stage. The mesocarp and columella tissues contained significantly fewer cells per unit
207 volume than the exocarp tissue. The cells from the exocarp tissue were small irregular polygons that were

208 compactly and densely arranged due to the cutin membrane, while the cells from the mesocarp and columella
209 tissues were large and sparsely and loosely arranged. Therefore, the failure stress and elastic modulus of exocarp
210 tissues are always exceed those of the internal mesocarp and columella tissues based on the biomaterial structure
211 and components, as reported by Li et al. (2012a) and Bargel & Neinhuis (2005).
212 Furthermore, the cell diameters in the tissues did not correlate with fruit ripeness in the experimental results.
213 During fruit development, slow cell division and enlargement occurs for 2~3 weeks, followed by rapid cell
214 enlargement for another 3~5 weeks. Subsequently, cell enlargement continues but will not significantly change
215 from the mature green stage (Thomas, 1996). Therefore, the cell size did not markedly differ between the six
216 ripening stages.

217 **3.3 Multi-scale biomechanics**

218 The results of the analysis of variance showed that the hardness, single cell mechanics and shear strength
219 of fruit at different scales (e.g. fruit, exocarp, mesocarp, columella and cell) were not significantly different
220 between the two cultivars. Therefore, one of the fruit cultivars, *Fendu 79*, was used as an example to illustrate
221 the multi-scale mechanical properties in this section.

222 **3.3.1 Multi-scale mechanical properties obtained from compression component**

223 The multi-scale mechanical properties of tomato fruits at six ripening stages obtained from compression
224 testing are given in Table 1. The ripening stage significantly affected the hardness of fruit at different scales. The
225 hardness of fruit at different scales negatively correlated with fruit ripeness. The hardness of whole fruits did not
226 significantly differ from that of exocarp tissue, and the hardness of exocarp tissue and its cells exceeded those of
227 the mesocarp and columella tissues and their cells. This finding illustrates that the exocarp tissue is the most
228 important factor for fruit hardness and would have a largest impact on the protection of internal tissues during
229 mechanical handling. Similarly, some puncture studies reported tomato hardness values on the order of 1~2 MPa
230 for six varieties of ripe fruit (Stommel, Abbott, Campbell, & Francis, 2005), decreases from 1.2 to 0.1 MPa for

231 mesocarp and columella tissues as the fruit ripened (Wu & Abbott, 2002), and values of 0.4~0.7 MPa for the
232 mesocarp and columella of ripe fruit punctured by probes of three sizes (Lana, Tijksens, Theije, Dekker, & Barrett,
233 2007). These published results are similar to those reported here. Furthermore, the difference in the hardness
234 between whole fruit and exocarp gradually decreased as the fruit ripened, which further illustrated that the
235 contribution of the exocarp to the hardness of whole fruit gradually increased as the fruit ripened. This viewpoint
236 is also supported by Jackman & Stanley (1994).

237 Hardness indicates the strength with which fruit can resist to external compression force. The transporter,
238 seller and consumer can use these forces to accurately evaluate the quality of postharvest fruit. In material science,
239 the hardness of metal and plastic materials is always measured based on a national standard method. However,
240 such a measurement method for biomaterials is currently lacking. The peak puncture force (Goyal, Kingsly,
241 Kumar, & Walia, 2007) and peak compression stress (Wu & Abbott, 2002) have been used to characterize the fruit
242 hardness in previous studies, and this approach differs from that utilized in this study. Therefore, comparing the
243 data presented herein with previously published results for further analysis is difficult.

244 In micro-scale research, the mean numbers of compressed cells in the exocarp, mesocarp and columella
245 tissue samples were 63553, 1614 and 1503, respectively. During the puncture test, the applied mean compression
246 force to single cells in the mesocarp and columella tissues was significantly larger than that experienced by single
247 cells in the exocarp tissue. The numbers of cells in the exocarp, mesocarp and columella tissue samples, which
248 directly contacted the probe end, were 11963, 115 and 106, respectively. The applied maximum compression force
249 to single cells in the mesocarp and columella tissues was at least 110 times larger than that applied to single cells
250 in the exocarp tissue. Some previous studies have reported bursting force ranges of single cells in ripe tomato
251 mesocarp tissue of 0~24 mN and a mean bursting force of 3.6 mN (Blewett, 2000). In contrast, the data in Table 2
252 show that the cells that directly contacted the probe end at the first several layers will burst, and their protoplasts
253 flow out during the puncture test. Conspicuously, a piece of tissue that was dropped into the counter bore

254 contained some damaged cells in its upper layer and some undamaged cells in its lower layer, and some liquids
255 remained on the end of the probe and the base plate after puncture.

256 **3.3.2 Multi-scale mechanical properties obtained from the shear component**

257 The multi-scale mechanical properties of tomato fruit at six ripening stages obtained from the shear
258 component are listed in Table 2. The shear strength of fruit at different scales significantly differed by the ripening
259 stage. The shear strength of fruit at different scales (e.g., fruit, exocarp, mesocarp, columella and cells) negatively
260 correlated with fruit ripeness. At the meso- and micro-scale, the shear strengths of the mesocarp and columella
261 tissues did not significantly differ, and the shear strength of the exocarp tissue and its single cells was an order of
262 magnitude larger than those of the mesocarp, columella tissues and their single cells. This finding illustrates that
263 the mesocarp, columella tissues and their single cells were prone to shear failure at a smaller external force than
264 the exocarp tissue and its single cells. Some previous studies reported shear strength values of light-red tomato
265 exocarp and mesocarp tissues of 2.98 ± 1.03 MPa and 0.07 ± 0.02 MPa, respectively, as determined by a shear
266 experiment (Li et al., 2012a). In contrast, Table 2 shows that shear strength values in mesocarp that are close to
267 these values, but shear strength values in the exocarp that are approximately 0.5 times. In micro-scale research,
268 the mean numbers of sheared cells in the exocarp, columella and mesocarp tissues were 2324, 603 and 584,
269 respectively. The applied mean shear force to single cells in the mesocarp and columella tissues was larger than
270 that applied to single cells in the exocarp tissue during a puncture test.

271 The shear strength, especially the maximum shear stress of biomaterials at failure (damage), is another
272 important characteristic of materials. This parameter can be helpful for the development of a fruit processing
273 machines, such as an auto-slicer; the design of packaging methods to prevent puncture damage during transporting;
274 and the textural assessment of crunchiness during chewing.

275 **4 Conclusions**

276 In this study, the multi-scale engineering properties of two tomato cultivars at six ripening stages were

277 simultaneously investigated. Our results show that the geometric mean diameter is the most suitable index to
278 predict fruit mass. A potential ripening scale based on the ratio of R:G:B obtained by quantifying the RGB value
279 for a given ripening stage has been proposed. The mechanical properties of tomato fruit, their tissues and their
280 single cells are heterogeneous and anisotropic due to the irregular shape and asymmetric internal structure at the
281 macro-scale, the non-unique tissue thickness at the meso-scale and the irregular change of size, shape and
282 arrangement of single cells at the micro-scale. The hardness and shear strength of fruit at different scales and the
283 single cell mechanics varied with the fruit ripening stage but not the chosen cultivars. The contribution of the
284 exocarp to the hardness of whole fruit gradually increased with fruit ripeness. This puncture experimental method
285 is well suited to measure the hardness and shear strength of multi-scale tomato fruit and the mechanics of single
286 tomato cells. The measured multi-scale engineering parameters are extremely important for intelligent harvesting,
287 multi-scale damage simulation and the postharvest textural evaluation of tomato fruits.

288 **Acknowledgments**

289 This work was supported by a Marie Curie International Incoming Fellowship within the 7th European
290 Community Framework Program (326847 and 912847) and the National Natural Science Foundation of China
291 (U1204107 and U1261115).

292 **References**

- 293 Arazuri, S., Jaren, C., Arana, J.I., & Perez De Ciriza, J.J. (2007). Influence of mechanical harvest on the physical
294 properties of processing tomato. *Journal of Food Engineering*, **80**(1), 190-198.
- 295 Bargel, H., & Neinhuis, C. (2005). Tomato fruit growth and ripening as related to the biomechanical properties of
296 fruit skin and isolated cuticle. *Journal of Experimental Botany*, **56**(413), 1049-1060.
- 297 Biswas, P., East, A. R., Hewett, E. W., & Heyes, J. A. (2014). Interpreting textural changes in low temperature
298 stored tomatoes. *Postharvest Biology and Technology*, **87**, 140-143.
- 299 Blewett, J.(2000). Micromanipulation of plant cell mechanical properties. PhD Thesis, University of Birmingham,

- 300 UK.
- 301 Chen, P., Hasegawaa, Y., & Yamashita, M. (2006). Grasping control of robot hand using fuzzy neural network.
- 302 *Lecture Notes in Computer Science*, **3927**, 1178-1187.
- 303 Dintwa, E., Jancsok, P., Mebatsion, H.K., Verlinden, B., Verboven, P., Wang, C.X., et al. (2011). A finite element
- 304 model for mechanical deformation of single tomato suspension cells. *Journal of Food Engineering*, **103**,
- 305 265-272.
- 306 Ghysels, P., Samaey, G., Van Liedekerke, P., Tijskens, E., Ramon, H., & Roose, D. (2010). Multiscale modeling of
- 307 viscoelastic plant tissue. *International Journal for Multiscale Computational Engineering*, **8**(4), 379-396
- 308 Genard, M., Bertin, N., Borel, C., Bussieres, P., Gautier, H., Habib, R., et al. (2007). Towards a virtual fruit
- 309 focusing on quality: modeling features and potential uses. *Journal of Experimental Botany*, **58**, 917-928.
- 310 Goyal, R.K., Kingsly, A.R.P., Kumar, P., & Walia, H. (2007). Physical and mechanical properties of aonla fruits.
- 311 *Journal of Food Engineering*, **82**, 595-599
- 312 Harker, F. R., Maindonald, J., Murray, S. H., Gunson, F. A., Hallett, I. C., & Walker, S. B. (2002). Sensory
- 313 interpretation of instrumental measurements 1: texture of apple fruit. *Postharvest biology and technology*, **24**(3),
- 314 225-239.
- 315 Hetzroni, A., Vana, A. & Mizrach, A. (2011). Biomechanical characteristics of tomato fruit peels. *Postharvest*
- 316 *Biology and Technology*, **59**, 80-84.
- 317 Ho, Q.T., Carmeliet, J., Datta, A.K., Defraeye, T., Delele, M.A., Herremans, E., et al. (2013). Multiscale modeling
- 318 in food engineering. *Journal of Food Engineering*, **114**, 279-291.
- 319 Kondo, N., Yata, K., Taniwaki, S., Tanihara, K., Monta, M., & Kurita, M. (2010). Development of an end-effector
- 320 for a tomato cluster harvesting robot. *Engineering in Agriculture, Environment and Food*, **3**(1), 20-24.
- 321 Lana, M.M., Tijskens, L.M.M., Theije, A.D., Dekker, M., & Barrett, D. M. (2007). Measurement of firmness of
- 322 fresh-cut sliced tomato using puncture tests – studies on sample size, probe size and direction of puncture.

- 323 *Journal of texture studies*, **38**, 601-618.
- 324 Li, Z.G., Li, P.P., & Liu, J.Z. (2011). Physical and mechanical properties of tomato fruits as related to robot's
325 harvesting. *Journal of Food Engineering*, **103**, 170-178.
- 326 Li, Z.G., Li, P.P., Yang, H.L., Liu, J.Z., & Xu, Y.F. (2012a). Mechanical properties of tomato exocarp, mesocarp
327 and locular gel tissues. *Journal of Food Engineering*. **111**, 82-91.
- 328 Li, C.S., Kan, Z., Tan, H.X., Zhang, R.Y., Sui, R.B., & Chen, D.F. (2012b). Development of 4FZ-30 self-propelled
329 tomato harvester. *Transactions of the CSAE*. **28**(10), 20-26.
- 330 Li, Z.G., Li, P.P., Yang, H.L., & Wang, Y.Q. (2013a). Stability tests of two-finger tomato grasping for harvesting
331 robots. *Biosystems Engineering*. **116**(2), 163-170.
- 332 Li, Z.G., Li, P.P., Yang, H.L., & Liu, J.Z. (2013b). Internal mechanical damage prediction in tomato compression
333 using multiscale finite element models. *Journal of Food Engineering*, **116**, 639-647.
- 334 Li, Z.G., & Thomas C.R. (2014a). Quantitative evaluation of mechanical damage to fresh fruits. *Trends in Food*
335 *Science & Technology*, **35**(2), 138-150.
- 336 Li, Z.G., & Thomas, C.R. (2014b). Multiscale biomechanics of tomato fruits: A review. *Critical Reviews in Food*
337 *Science and Nutrition*. DOI:10.1080/10408398.2012.759902
- 338 Jackman, R.L., & Stanley, D.W. (1994). Influence of the skin on puncture properties of chilled and nonchilled
339 tomato fruit. *Journal of Texture Studies*. **25**, 221-230.
- 340 Mebatsion, H.K., Verboven, P., Ho, Q.T., Verlinden, B.E., & Nicolai, B.M. (2008). Modeling fruit (micro)
341 structures, why and how? *Trends in Food Science & Technology*, **19**, 59-66.
- 342 Monta, M., Kondo, N., & Ting, K.C. (1998). End-effectors for tomato harvesting robot. *Artificial Intelligence*
343 *Review*, **12**, 11-25.
- 344 Rancic, D., Quarrie, S., & Pecinar, I. (2010). Anatomy of tomato fruit and fruit pedicel during fruit development.
345 *Microscopy: Science, Technology, Applications and Education*. **2**, 851-861.

- 346 Saladie, M., Matas, A.J., Isaacson, T., Jenks, A.S., Goodwin, S.M., Niklas, K.J., et al. (2007). A reevaluation of the
347 key factors that influence tomato fruit softening and integrity. *Plant Physiology*, **144**, 1012-1028.
- 348 Salunkhe, D.K., Jadhav, S.J., & Yu, M.H., (1974). Quality and nutritional composition of tomato fruit as
349 influenced by certain biochemical and physiological changes. *Qualitas Plantarum*, **24**, 85-113.
- 350 Sirisomboon, P., Tanaka, M., & Kojima, T. (2012). Evaluation of tomato textural mechanical properties. *Journal*
351 *of Food Engineering*, **111**, 618-624.
- 352 Stommel, R.J., Abbott, J.A., Campbell, T.A., & Francis, D. (2005). Inheritance of elastic and viscoelastic
353 components of tomato firmness derived from intra- and interspecific genetic backgrounds. *Journal of the*
354 *American Society for Horticultural Science*, **130**, 598-604.
- 355 Thomas L.R. (1996). <http://www-plb.ucdavis.edu/labs/rost/tomato/Reproductive/anat.html>.
- 356 Tanigaki, K., Fujiura, T., Akase, A., & Imagawa, J. (2008). Cherry harvesting robot. *Computers and Electronics in*
357 *Agriculture*, **63**, 65-72.
- 358 USDA (1991). <http://www.ams.usda.gov/AMSV1.0/getfile?dDocName=STELPRDC5050331>.
- 359 Van Linden, V., Scheerlinck, N., Desmet, M., & De Baerdemaeker, J. (2006). Factors that affect tomato bruise
360 development as a result of mechanical impact. *Postharvest Biology and Technology*, **42**, 260-270.
- 361 Wu, T., & Abbott, J.A. (2002). Firmness and force relaxation characteristics of tomatoes stored intact or as slices.
362 *Postharvest Biology and Technology*, **24**, 59-68.

363

364

365 **Figure and Table Captions**

366

367 **Figure 1** - Tomato fruits at six ripening stages and their corresponding RGB values.368 **Figure 2** – Multi-scale geometrical characteristics of tomato fruits.369 **Figure 3** - Puncture test of tomato fruits and the calculation of the mechanical parameters.370 **Figure 4** - Geometric characteristics of tomato fruits at the macro level.371 **Figure 5** - Cell diameters in different types of tissues of two tomato cultivars with microstructure pictures.372 **Table 1** Multi-scale mechanical properties of *Fendu 79* tomato fruit obtained from compression testing.373 **Table 2** Multi-scale mechanical properties of *Fendu 79* tomato fruit obtained from shear testing

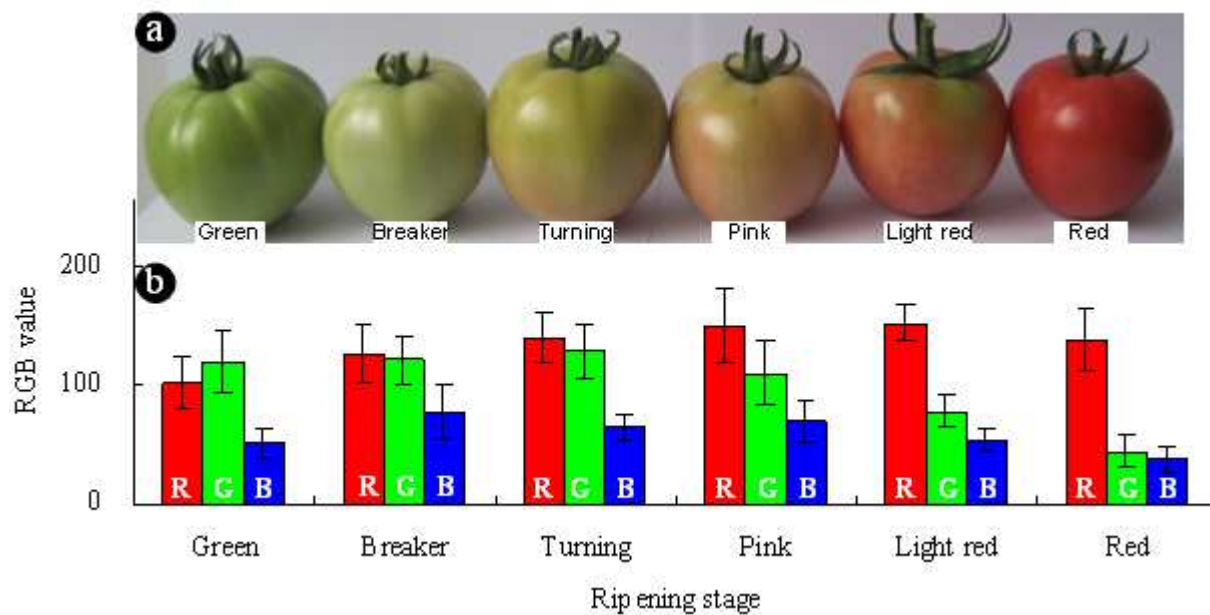
374

375 **Figure 1**

376

377

378



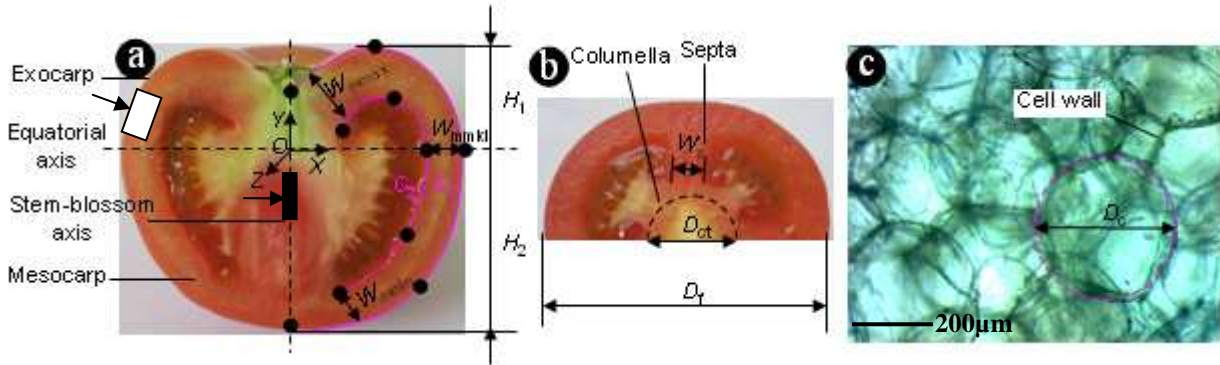
379

380 **Fig. 1** Tomato fruits at six ripening stages and their corresponding RGB values. (a) Six ripening stages of tomato

381 fruits. (b) RGB values of tomato fruits at the six ripening stages, R-Red, G-Green, B-Blue. Data are expressed as

382 the mean \pm SD ($n=10$).

383

384 **Figure 2**385
386
387
388
389

390

391 **Fig. 2** Multi-scale geometrical characteristics of tomato fruits. (a) Longitudinal section of a tomato fruit along the
 392 stem-apex axis. The white rectangle shows the sampling zone in exocarp and mesocarp tissue, and the arrow is
 393 pointing to the angle of observation. The black rectangle shows the sampling zone in columella tissue, and the
 394 arrow shows the angle of observation. (b) Transverse equatorial half-section of a tomato fruit. (c) Cells in the
 395 columella tissue of breaker tomato fruit. H_1 -Height above the fruit's equatorial axis, H_2 -Height below the fruit's
 396 equatorial axis, D_f -Diameter of the equatorial section, W_{max} , W_{min} and W_{mid} - Maximum, minimum and middle
 397 thickness of the mesocarp tissue, W_s -Thickness of the septa tissue, D_{ct} -Columella diameter, D_c -Cell diameter.

398

399

400
401
402

Figure 3

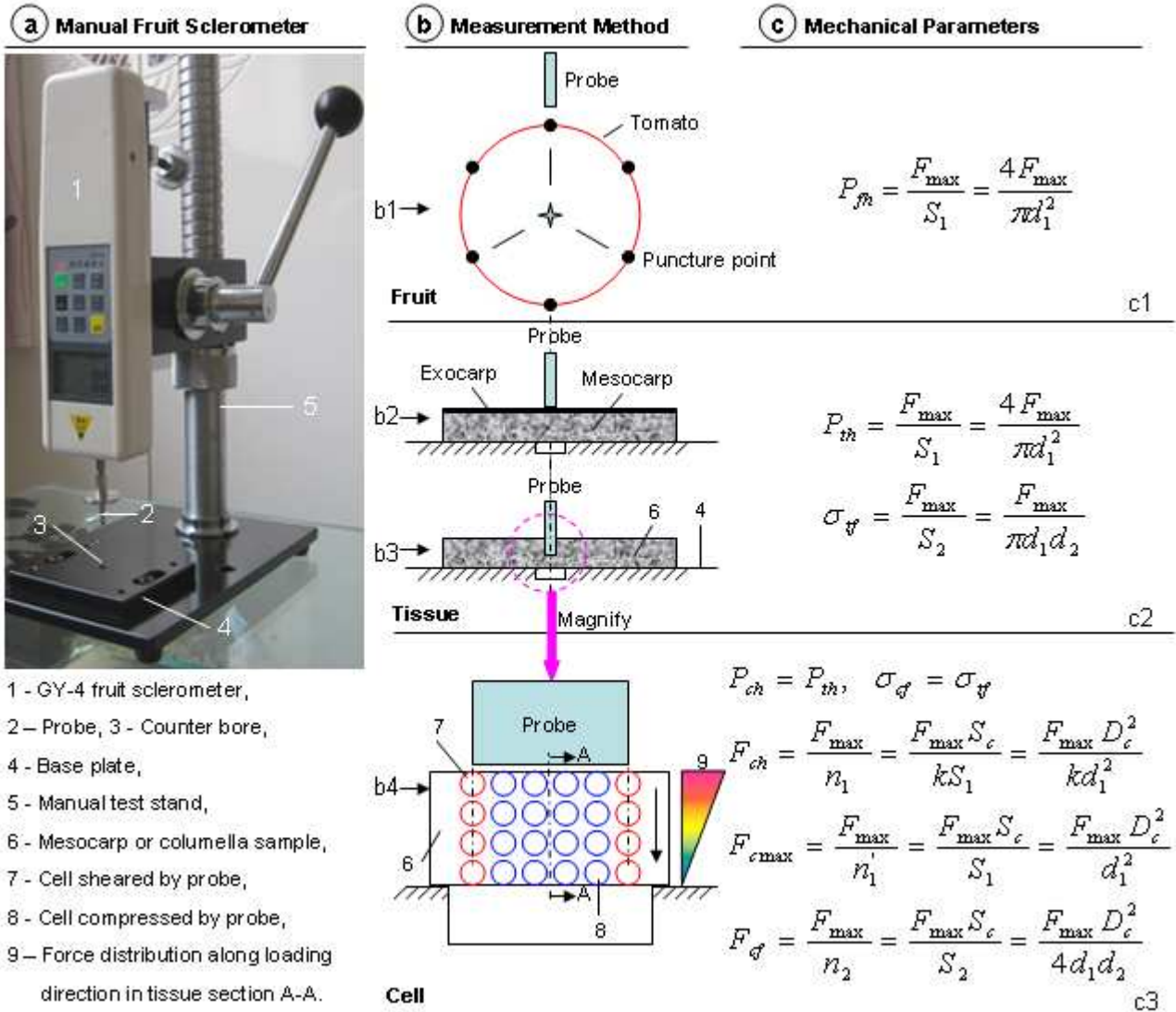
403
404
405
406
407
408
409
410
411
412
413
414
415
416

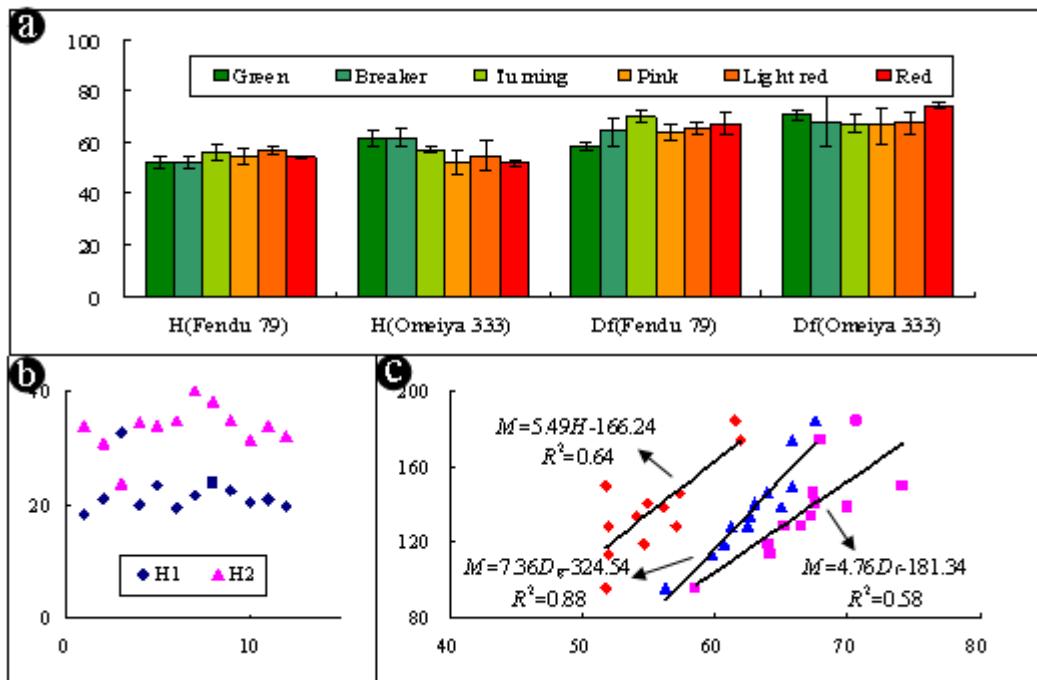
Fig. 3 Puncture test of tomato fruits and the calculation of the mechanical parameters. P_{fn} , P_{th} and P_{ch} are the hardness of fruits, tissues and single cells, respectively, subjected to probing; $\sigma_{\mathcal{F}}$ and σ_{cf} are the shear strength of tissues and single cells subjected to probing; F_{\max} is the applied peak puncture force of the probe; F_{ch} is the applied mean compression force to single cells during the puncture test; $F_{c\max}$ is the applied maximum compression force to single cells during the puncture test; $F_{\mathcal{F}}$ is the applied mean shear force to single cell during the puncture test; S_1 and S_2 are the valid compression and shear areas, respectively; D_c and S_c are the diameter and equatorial section areas of a cell; d_1 and d_2 are the probe diameter and tissue sample thickness, respectively; n_1 and n_2 are the numbers of cells compressed by probe and sheared by probe, respectively, and k is the number of cell layers ($k = d_2/D_c$); n'_1 is the number of first-layer cells compressed by the probe.

417 **Figure 4**

418

419

420



421

422

423

424

425

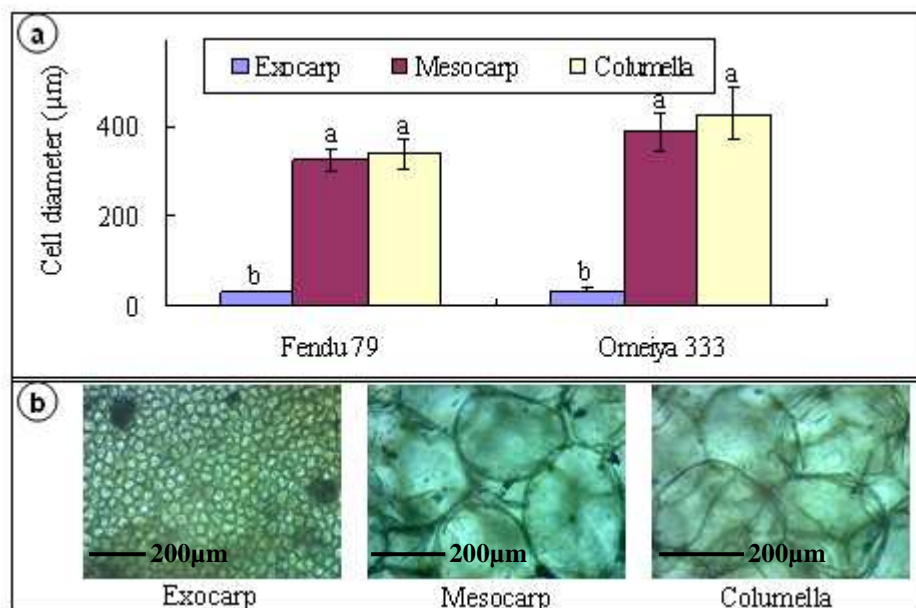
426

427

428

Fig. 4 Geometric characteristics of tomato fruits at the macro level. (a) Heights and Equatorial diameters of tomato fruits at the six ripening stages, ordinate unit: mm. H -Fruit height, D_f -Equatorial diameter. Data are expressed as the mean \pm SD ($n=5$). (b) Fruit height above or below the equatorial section, ordinate unit: mm, abscissa unit: number. $H1$ -Fruit height above the equatorial section, $H2$ -Fruit height below the equatorial section. (c) Regression relationships between M and H , D_f , D_g , respectively. M -fruit mass, D_g -geometric mean diameter, ordinate unit: g, abscissa unit: mm.

Figure 5



433 **Fig. 5** Cell diameters in different types of tissues of two tomato cultivars and microstructural pictures. (a) Cell
 434 diameters of *Fendu 79* and *Omeiya 333* tomato fruits. Data are expressed as the mean \pm SD ($n=5$). For each
 435 variety, the letters above the error bar indicate significant differences ($P < 0.05$) according to Student's t -test. (b)
 436 Microstructure of exocarp, mesocarp and columella tissues of *Fendu 79* tomato fruits at the breaker stage
 437

453 **Table 2**

454

455

Table 2 Multi-scale mechanical properties of *Fendu 79* tomato fruit resulted from shear component

Multi-scale	Biomaterials	Ripening stage					
		Green	Breaker	Turning	Pink	Light red	Red
ANOVA: Multiple-comparison		a	ab	abc	abc	bc	c
Meso-/Micro-Scale (MPa)	Exocarp [*]	11.58±1.20	10.12±0.38	9.63±0.48	7.44±0.44	5.89±0.54	5.78±0.85
	Mesocarp ^{**}	0.26±0.03	0.25±0.02	0.24±0.03	0.16±0.06	0.09±0.01	0.06±0.03
	Columella ^{**}	0.33±0.04	0.15±0.01	0.14±0.01	0.11±0.03	0.10±0.01	0.04±0.01
Micro-scale (mN)	Cell in exocarp ⁺	9.31±0.97	7.82±0.30	7.74±0.39	5.98±0.35	4.73±0.44	4.65±0.68
	Cell in mesocarp ⁺⁺	21.82±2.60	20.77±1.84	20.14±2.15	13.34±5.14	6.70±1.12	5.37±2.39
	Cell in columella ⁺⁺	29.99±3.30	13.94±1.28	13.03±0.63	10.26±2.86	9.01±0.88	4.06±0.83

456 Data are expressed as the mean \pm SD ($n=3$). Different letters (namely a, ab, abc, bc, c) in the same row indicate
 457 significant difference ($P < 0.05$) according to Student's t -test. The superscript marks (*) in the meso-scale column
 458 indicate significant differences ($P < 0.05$), and the superscript marks (+) in the micro-scale column indicate
 459 significant differences ($P < 0.05$).

460 σ_{tf} and σ_{cf} are the shear strength of tissues and single cells subjected to probing; F_{cf} is the applied mean shear force
 461 to a single cell during the puncture test.

462

Highlights

- ◆ Geometric mean diameter was most closely correlated with tomato fruit mass
- ◆ Multi-scale geometry of tomatoes showed heterogeneous and anisotropic properties
- ◆ The contribution of exocarp to the hardness of whole fruit increased with ripeness
- ◆ Puncture experiment is suited to measure the multi-scale mechanics of fruit